Cinchonidine Adsorption on Gold and Gold-Containing Bimetallic Platinum Metal Surfaces: An Attenuated Total Reflection Infrared and Density Functional Theory Study

Bahar Behzadi,[†,‡] Angelo Vargas,[†] Davide Ferri,[†] Karl-Heinz Ernst,[‡] and Alfons Baiker*[,†]

Department of Chemistry and Applied Biosciences, Institute for Chemical and Bioengineering, ETH Zurich, HCI, CH-8093 Zurich, Switzerland, and Nanoscale Materials Science, Empa, Swiss Federal Laboratories for Materials Testing and Research, CH-8600, Dübendorf, Switzerland

Received: April 7, 2006; In Final Form: June 20, 2006

Adsorption of cinchonidine on monometallic Au and bimetallic Pt−Au and Pd−Au thin model films prepared by physical vapor deposition has been investigated with attenuated total reflection infrared (ATR-IR) spectroscopy. On Au the alkaloid forms an adsorbed layer that shows higher stability against desorption than the corresponding adsorption on Pt. In this adsorption layer the intermolecular interactions dominate over metal−adsorbate interactions as indicated by the absence of the spectroscopic features attributed to strongly flat adsorbed species. This behavior is further supported by Density Functional Theory (DFT) calculations indicating that flat and tilted orientations of the quinoline ring have comparable adsorption energy on Au but lower (7−10 kcal/mol) compared to adsorption on Pt (ca. 40 kcal/mol). As a consequence, the creation of a metal surface with isolated chiral sites is prevented by formation of an adsorbed structure formed by intermolecularly bound cinchonidine molecules on Au. While the binding to Pt is due to the formation of σ-bonds to surface atoms, such aggregates are bound to Au mainly by van der Waals forces. Given this different nature of bonding of cinchonidine to Au and Pt, addition of Au to Pt and Pd films could be used to probe the changes of fractional coverage of the different adsorbed species of cinchonidine on the platinum metals. It is demonstrated that the lowering of the domain size of the platinum group metal by Au can simulate the effect of particle size on the distribution of the surface conformations of the alkaloid on a metal surface.

Introduction

Among various other applications in chemical synthesis,[1] cinchona alkaloids are efficient chiral additives whose adsorption on platinum-group metal surfaces produces chirally modified metal catalysts highly active in the enantioselective hydrogenation of activated ketones and olefins.[2,3] Upon adsorption of the modifier on the metal a three-dimensional chiral space (*chiral pocket*) constrained by the surface and the skeleton of the modifier is generated.[4] A key feature of this adsorption process is the formation of chiral sites by single adsorbed molecules. The shape of the chiral space that has to be properly matched by the substrate to be hydrogenated is a decisive factor for the control of enantioselection[5,6] and is strongly affected by the way the modifier is anchored to the surface.

Adsorption of cinchonidine and derivatives on Pt has been studied with several spectroscopic techniques[6−12] and electrochemical methods.[13,14] STM studies indicated that adsorption is disordered on catalytically relevant metals and provided direct evidence for the single molecule site-type of chirality.[15,16] There is general agreement on the adsorption behavior of cinchonidine on Pt, which is affected by coverage,[9,17] temperature,[8,18] and probably solvent[19] and pressure. Additionally, the rich conformational behavior of the cinchona alkaloids complicates considerably the adsorption process as suggested by the number of feasible surface conformations.[4,20,21] Three adsorbed species have been identified on Pt with infrared spectroscopy. Though there is indication that the quinuclidine-N atom may contribute to the adsorption strength of cinchonidine,[6,20,22] the dominant interaction with the surface is given by the quinoline ring. At low coverage a preferential geometry with the aromatic ring nearly parallel to the surface is favored, whereas the ring tilts away from the surface plane with increasing surface crowding (Figure 1). A third edge-on species was proposed to originate from α-H abstraction (α-quinolyl).[9] The strength of adsorption decreases qualitatively in the series flat > α-quinolyl > tilted. Adsorption of the nearly flat adsorbed species has been modeled with DFT[4] and molecular dynamics[22] methods. Recently, the tilted species has also been shown to be over 20 kcal/mol less strongly adsorbed than the flat species.[21]

Interaction of Pd with cinchonidine generates an adsorbed layer less strongly bound to the metal in which the dominant local adsorption geometry is likely close to the tilted one shown in Figure 1. The tilting of the quinoline ring has been corroborated under both UHV[23] and ambient conditions.[24]

Given the different strength of interaction of cinchonidine demonstrated on Pt and Pd, and its influence on the outcome of enantioselectivity in enantioselective hydrogenations, it seems interesting to modulate the adsorption behavior of the chiral modifier by changing the surface composition of a bimetallic catalyst. Although Pt−Pd catalysts have been tested in the enantioselective hydrogenation of ethyl pyruvate and ketopantolactone,[25] to date the adsorption of cinchona alkaloids has not been studied on bimetallic surfaces. The main reason for the lower activity and selectivity of Pt−Pd catalysts compared to Pt was traced to the ensemble effect induced by deposition of Pd on Pt, which changes the optimal adsorption geometry of the modifier.

* Address correspondence to this author. E-mail: baiker@chem.ethz.ch. Fax: +41-044-632-1163.
[†] Institute for Chemical and Bioengineering, ETH Zurich.
[‡] Swiss Federal Laboratories for Materials Testing and Research.

10.1021/jp062174u CCC: $33.50
Published on Web 08/10/2006

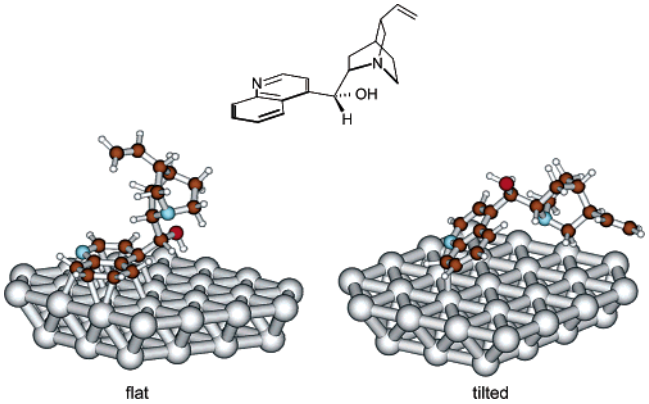

Figure 1. Molecular structure of cinchonidine and view on the local geometry of adsorbed species on Pt. Computational details of the two structures are given in refs 20 and 21 where they have been named SO3 and T1, respectively. The tilted species was also spectroscopically observed on Pd (see text for details). No calculated structure is available for the third species (α-quinolyl) proposed in ref 9.

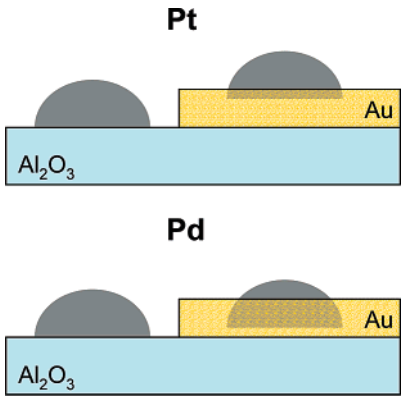

Figure 2. Schematic presentation of the proposed model for monometallic and bimetallic surfaces used in this study.

Despite the fact that gold shows poor hydrogenation activity,[26,27] it appears an interesting metal to be combined with Pt and Pd. The main reason for using Au to probe the effect of bimetallic surfaces on cinchonidine adsorption is its suitability to change the "ensemble size" of the platinum group metal[28,29] and thereby activity and selectivity of hydrogenation catalysts. Both alloying as well as simple "blocking" of active surface metal atoms influence (reduce) the size of the ensembles of the platinum group metal. Hence, binary Pt−Au and Pd−Au films represent interesting model surfaces for investigating the structure sensitivity of cinchonidine adsorption on platinum group metals. A similar approach has been applied to Ni−Au alloys to investigate the adsorption of methylacetoacetate[30] and tartaric acid[31] used in the enantioselective hydrogenation over Ni catalysts as substrate and chiral modifier, respectively.[32]

Here the adsorption of cinchonidine on Pt−Au and Pd−Au thin model films has been studied by using attenuated total reflection infrared (ATR-IR) spectroscopy. These films revealed interesting surface properties since evaporation of Au generates a diffuse interface, which reduces the effective size of Pd and Pt ensembles (Figure 2).[33] The adsorption was followed in the presence of CH_2Cl_2 solvent and dissolved hydrogen. Density functional theory calculations of the adsorption of quinoline on platinum and gold clusters are also reported as models for the adsorption of cinchonidine, as a complement to the experimental information on the relative adsorption strength.

Experimental Section

Materials. Cinchonidine (Fluka, 98%) was used as received. Dichloromethane solvent (Baker) was stored over 5-Å molecular sieves. N_2 (99.995 vol %) and H_2 (99.999 vol %) were supplied by PANGAS. Pt (99.99%), Pd (99.95%), and Au (99.99%) wires and Al_2O_3 (99.3%) tablets used as a target for electron beam vapor deposition were supplied by Unaxis.

Thin Film Preparation. Trapezoidal Ge internal reflection elements (IRE, 50 × 20 × 2 mm^3, Komlas) were coated with 100 nm of Al_2O_3 and then with one or two thin metallic films. Coatings were prepared in a BAE-370 (Balzers) vacuum system by evaporation of target materials from a graphite crucible (8 kV and up to 0.15 mA) at a maximum base pressure of 1×10^{-5} mbar and typical evaporation rates of 0.5 and 1.0 Å/s for metallic and Al_2O_3 films, respectively. The film thickness was measured with a quartz microbalance. The evaporation unit was equipped with a 4-pocket turret allowing consecutive deposition of materials without breaking the vacuum.

The following designations are used for the monometallic and bimetallic samples. Monometallic samples are denoted as M*x*, where M is either Pt, Pd, or Au, and *x* is the metal film thickness in Å units (10, 20, and 10, respectively). When Pt or Pd was deposited on 1 nm of Au in addition to Al_2O_3, samples were designated as MAu02, MAu05, MAu10, and MAu20, according to the amount of deposited noble metal. The designation PtAu and PdAu throughout the text does not imply alloy formation.

Figure 2 depicts a model of the bimetallic surface compared to Pt[9] and Pd[24] films according to the characterization based on CO adsorption from the liquid phase.[33] A diffuse interface is readily formed on PdAu surfaces, whereas the two metals appear more segregated on the PtAu surfaces.

ATR-IR Spectroscopy. ATR-IR spectra of the solid−liquid interface were recorded in situ on an EQUINOX 55 spectrometer (Bruker Optics) equipped with a liquid nitrogen-cooled MCT detector by co-adding 200 scans at 4 cm^{-1} resolution. The coated Ge crystal was mounted in a homemade stainless steel flow-through cell, which was maintained at 10 °C throughout the experiments. The experimental procedure for adsorption studies is analogous to that reported previously.[34] Briefly, after stabilization of the system under flowing N_2-saturated CH_2Cl_2, the metal coating was contacted with H_2-saturated CH_2Cl_2 for about 10 min, the time required to create large Pt domains. A spectrum was then recorded that served as background for the next spectra. A solution of cinchonidine (0.1 mM) was then admitted to the cell and ATR-IR spectra were collected as a function of time. The solution of the alkaloid was replaced by H_2-saturated CH_2Cl_2 after about 60 min on stream to remove weakly adsorbed and dissolved species.

All experiments were performed at a flow rate of ca. 1.0 mL/min. Spectra are presented in absorbance units. Where needed, water vapor was subtracted from the spectra. Peak integration was performed with the OPUS 5.0 software package.

Theoretical Calculations. Adsorption studies have been performed with the Amsterdam Density Functional (ADF) program package.[35] The surface was simulated by using rigid Pt 31 and Au 31 clusters. The following level of theory was used: orbitals up to 1s were kept frozen for the second row elements, while orbitals up to 4f were kept frozen for Pt and Au; the double-ζ (DZ) basis functions were used for platinum and gold, while for second row elements and hydrogen double-ζ plus polarization (DZP) basis functions were used; Zero Order Regular Approximation was used for the relativistic Hamiltonian,[36−40] and Dirac core potentials for all atoms;[35]

TABLE 1: Assignment of the Principal Vibrational Modes of Cinchonidine on Pt, Pd, and Au Surfaces According to Previous ATR-IR Studies and the Present Work[a]

assignment			adsorbed		
mode	species	solution[b]	Pt	Pd	Au
ring str + δ(CH), Q		1383	n.o.[c]	n.o.[c]	1375
ring def, Q	tilted	1423	n.o.[c] (1421)[d]	n.o.[c]	1420
δ(CH), Qd	all	1454	1458	1456	1452
ring def, Q	tilted	1509	1511	1509	1508
ring def, Q	α-quinolyl		1530	n.o.	n.o.
ring def, Q	flat[e]	1570	1570	1567	1570
ring def, Q	tilted	1593	1590	1586	1589
ring def, Q	tilted	1615	1610	1612	n.o.
ν(C=C), vin		1635	n.o.[f]	n.o.[f]	n.o.

[a] The values for free cinchonidine are also given for comparison. ν = stretching; δ = bending; str = stretching; def = deformation; Qd = quinuclidine moiety; Q = quinoline moiety; vin = vinyl group; n.o., not observed. [b] IR spectrum of a 0.01 M solution in CH_2Cl_2. [c] Because of interference of the strong negative signal at ca. 1400 cm^{-1} due to removal of CH_x-like species upon adsorption (cleaning effect). [d] Observed only for adsorption from cyclohexane solvent (see ref 9). [e] The signal is in principle common to all species but explicitly represents the flat species on metals (Pt), where its intensity exceeds that of the signal at ca. 1590 cm^{-1} (see text). [f] The vinyl group is readily hydrogenated upon contact with these metals.

Becke-Perdew exchange and correlation corrections were used in the density functional.[41,42] A more detailed description of the computational methods used can be found elsewhere.[20,21] All calculations were run unrestricted. Adsorption energies (E_{ads}) were calculated as follows:

$$\Delta E_{ads} = E_{cluster+adsorbate} - E_{cluster} - E_{free\ molecule}$$

where $E_{cluster}$ is the single point energy of the rigid cluster, $E_{cluster+adsorbate}$ is the optimized energy of the adsorbate on the rigid cluster, and $E_{adsorbate}$ is the optimized geometry of the isolated adsorbate. Geometry optimizations are based on a quasi-Newton−Raphson approach,[43,44] and the Hessian updating scheme used is BFGS (Broyden−Fletcher−Goldfarb−Shanno). Convergence criteria applied are 10^{-3} hartrees for the energy, 10^{-2} hartrees/Å for the gradients, and 10^{-2} Å for the coordinates. All calculations were run at 0 K.

For benzene on platinum it was shown that the addition of the BSSE correction and of partial relaxation of the metal cluster led to contributions of opposite sign which tend to compensate, and that the simple formula used leads to values for the adsorption strength close to the experimental value for both bridge and hollow sites.[45]

The bond distances for Pt and for Au were fixed to the experimental value of 2.775 and 2.870 Å for bulk metal.[46] Molden[47] was used as the graphical interface.

Results

Previous studies on the adsorption of cinchonidine on platinum[9,11,17] and palladium[24] have revealed several features that are important for interpreting the ATR-IR spectra measured on Au, PtAu, and PdAu surfaces. The characteristic signals of the species typically observed with ATR-IR spectroscopy on platinum metal surfaces are reviewed in Table 1 for the spectral region of interest. The main difference between flat and tilted species in terms of infrared signals is the resemblance of the spectrum associated to the latter species with the spectrum of cinchonidine in solution. This observation indicates that tilted adsorption does not substantially perturb the molecular structure of the alkaloid. On the other hand, the change upon adsorption of the relative intensity of the signal at 1569 cm^{-1} in solution

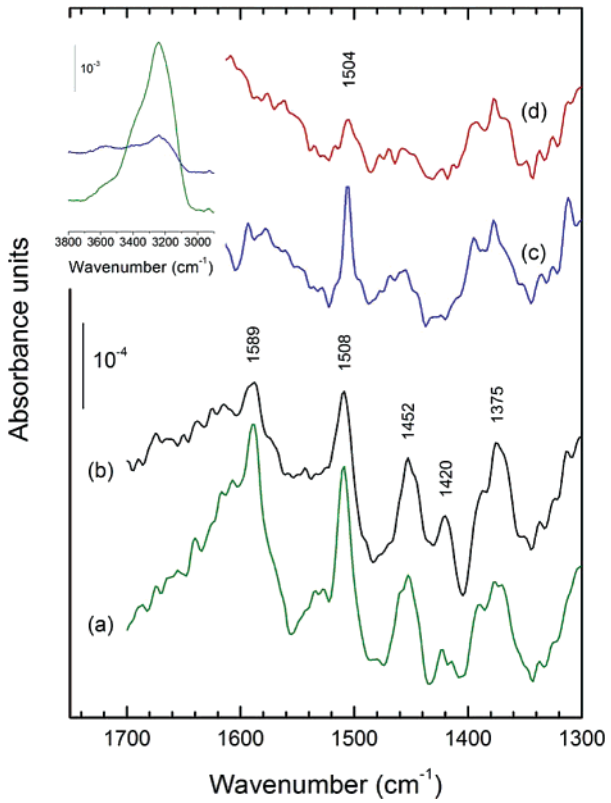

Figure 3. ATR-IR spectra of (a) cinchonidine and (c) quinoline on monometallic Au. Spectra b and d correspond to the state of the adsorbed layer after H_2-saturated solvent flow for about 30 min. The inset shows the 3800−2900 cm^{-1} spectral region of spectra a and c. Conditions: t = 60 min, C = 0.1 mM, 10 °C, H_2-saturated CH_2Cl_2.

with respect to that for example at 1509 cm^{-1} indicates that the former signal describes a species (flat) in which the quinoline ring is perturbed by the presence of the metal, as demonstrated by theoretical calculations.[4]

Cinchonidine on Au. The spectrum of cinchonidine on Au10 (Figure 3a) exhibits signals at 1590, 1508, 1452, 1420, and 1376 cm^{-1}. Two signals (not shown) at 2919 and 2854 cm^{-1} which appear better resolved than on Pt are characteristic of C−H stretch modes of the quinuclidine moiety. Only a very weak signal is observed at ca. 1570 cm^{-1}, otherwise the spectrum indicates that cinchonidine adsorbs on gold predominantly in a tilted mode. Although the positions of the signals attributed to the tilted mode on the different metals do not substantially differ (Table 1), on Au this adsorption mode cannot be properly named "tilted" as it is on Pt and Pd. This point will be addressed in the Discussion.

The absence of the negative signal at 1400 cm^{-1} enables the observation of modes at 1420 and 1375 cm^{-1}, corresponding to ring deformation and stretch modes, respectively, with a strong contribution from in-plane C−H deformation.[9,12] These modes have a component normal to the metal surface and hence are infrared active only when the quinoline ring points away from Au. The observation of these modes and the absence of a clear signal at ca. 1570 cm^{-1} substantiate the dominance of species in which the quinoline ring is strongly tilted with respect to the Au surface. These spectroscopic features should be characteristic of weak adsorption of cinchonidine. On the contrary, the cinchonidine adsorbate shows higher stability against desorption compared to Pt.

The origin of this behavior was studied by separately investigating the adsorption of quinoline, the anchoring group on platinum metals. Figure 3c,d shows that quinoline desorbs

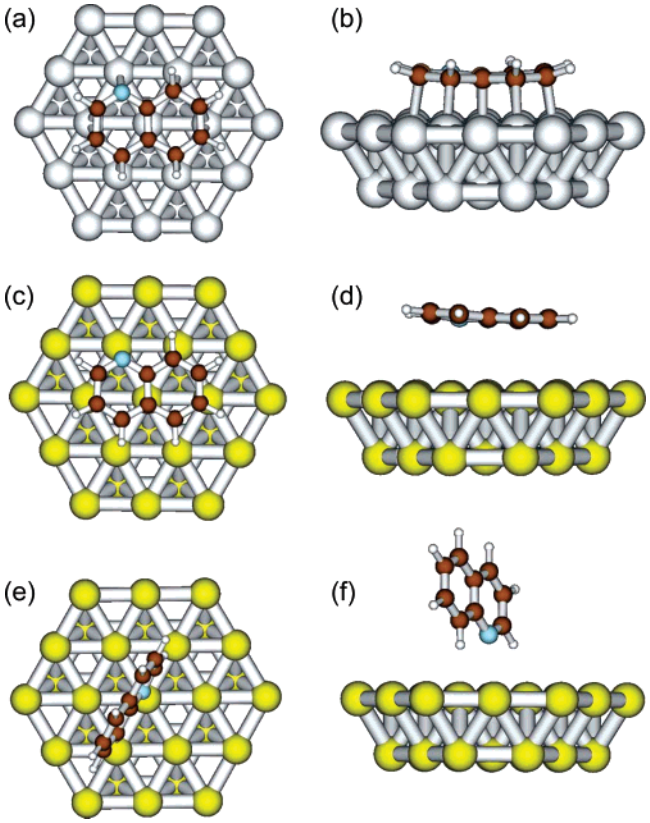

Figure 4. Calculated structures for quinoline adsorbed with the aromatic ring on Pt (a, b) and Au (c, d) clusters, and with the N lone pair on the Au (e, f) cluster. Adsorption energies are 40.4, 6.9, and 9.1 kcal/mol, respectively.

from Au to a greater extent than cinchonidine but not completely as a result of the solvent flow. The features appearing during cinchonidine adsorption are more complex and exhibit higher intensity than those of quinoline thus accounting for a relatively denser adsorbate layer. Similarly, the intensity of the signals of cinchonidine on Au is by a factor 3 lower than that on Pt (see below). The absence of the signal at ca. 1590 cm^{-1} in the case of quinoline strongly suggests a different interaction of the aromatic ring of the two molecules with Au, which contrasts with the similarity of the adsorption behavior of these molecules on Pt and Pd.[9,24]

In the spectra of both quinoline and cinchonidine on Au, a prominent signal appears at ca. 3240 cm^{-1} that is about eight times more intense for the alkaloid (inset of Figure 3). The signal can be assigned to the restructuring of the water layer present on Au before adsorption since it is observed with quinoline as well.

To gain further insight, the adsorption of quinoline on Au(111) was simulated by using relativistically corrected Density Functional Theory (DFT) and the results are shown in Figure 4. The adsorption energies calculated for flat-like species were found to be 40.4 and 6.9 kcal/mol on Pt and Au, respectively. It is obvious from these values that quinoline is essentially physisorbed on Au, whereas it is chemisorbed on Pt. Furthermore, the adsorption site is shifted from a bridge site on Pt to a site showing a nonspecific interaction to Au atoms. Table 2 gives the values of bond lengths for quinoline in a vacuum and adsorbed with the aromatic ring approximately parallel to Pt and Au, whereas Table 3 lists the values of the angles between the hydrogen atoms and the aromatic skeleton. Deviation from the structure in a vacuum indicates strong interaction with the metal. Au(111) leaves the structure of quinoline practically

TABLE 2: Values of Bond Distances Calculated for Free Quinoline and for the Adsorption of Quinoline on Pt and Au on a Double Bridge Site[a]

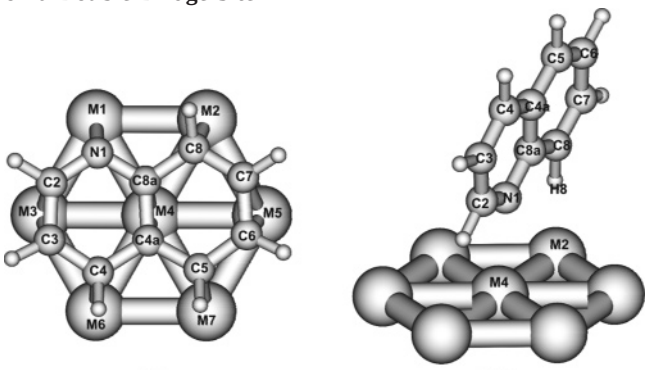

		adsorbed		
		flat		tilted
	free	Pt	Au	Au
N1−C2	1.32	1.37	1.32	1.32
C2−C3	1.41	1.43	1.41	1.41
C3−C4	1.37	1.47	1.37	1.37
C4−C4a	1.41	1.48	1.42	1.41
C4a−C5	1.41	1.48	1.42	1.42
C5−C6	1.37	1.47	1.38	1.38
C6−C7	1.41	1.42	1.41	1.41
C7−C8	1.37	1.46	1.38	1.38
C8−C8a	1.41	1.48	1.42	1.41
C8a−C4a	1.43	1.48	1.43	1.43
N1−M1		2.38	3.37	
C2−M3		2.38	3.72	
C3−M3		2.25	3.58	
C4−M6		2.24	3.84	
C4a−M4		2.16	3.33	
C8a−M4		2.19	3.51	
C5−M7		2.24	3.70	
C6−M5		2.25	3.27	
C7−M5		2.34	3.52	
C8−M2		2.26	3.26	
N1−M4				2.81
H8−M2				2.41

[a] The atom numbering is given in the top panel. All values are in Å.

TABLE 3: Values of Dihedral Angles between Hydrogen Atoms and the Quinoline Ring Skeleton Calculated for the Adsorption of Quinoline on Pt and Au[a]

	flat		tilted
	Pt	Au	Au
H−C2−N1−C3	171	180	180
H−C3−C2−C4	159	180	180
H−C4−C3−C4a	139	180	180
H−C5−C4a−C6	138	179	180
H−C6−C5−C7	161	179	180
H−C7−C6−C8	168	180	180
H−C8−C7−C8a	138	177	180

[a] Atom numbering reference is in Table 2. All values are in degrees.

unaltered, therefore binding quinoline only weakly, whereas Pt(111) strongly interacts with the heterocyclic ring system. Rehybridization of the aromatic carbon atoms does not take place on Au (Table 3), and the distance to the metal increases by more than 1 Å with respect to adsorption on Pt (Table 2). The bond distances in the carbon skeleton remain practically unchanged on Au compared to the compound in a vacuum. Interestingly, adsorption of quinoline with the aromatic ring nearly perpendicular to the Au(111) surface, as shown in Figure 4, is characterized by an adsorption energy of 9.1 kcal/mol, which is only slightly higher than that of the flat-like species.

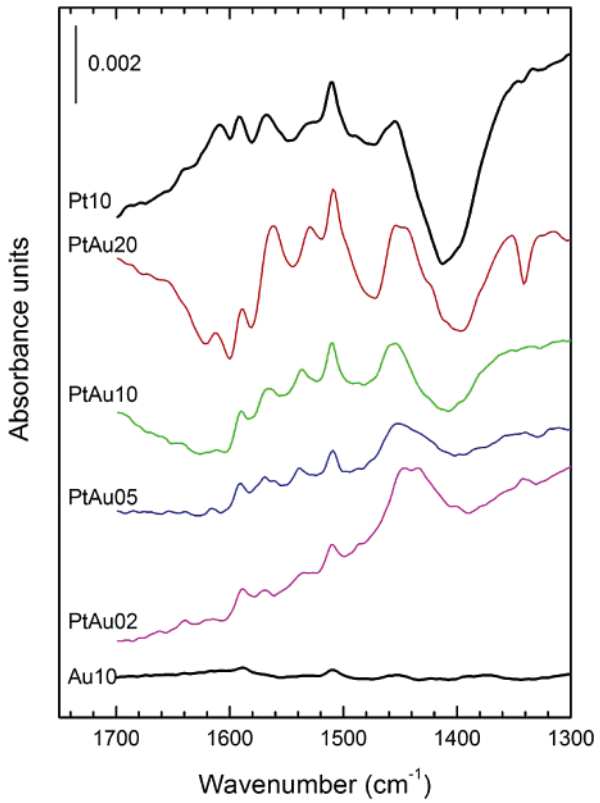

Figure 5. ATR-IR spectra of cinchonidine on monometallic Au and Pt (bold) and on bimetallic PtAu. Conditions: $t = 60$ min, $C_{CD} = 0.1$ mM, 10 °C, H_2-saturated CH_2Cl_2.

This is an important observation because other factors such as intermolecular forces can become important thus controlling the adsorption state of cinchonidine on Au.

Cinchonidine on PtAu and PdAu Surfaces. The ATR-IR spectra recorded after contact of the surface with a solution of cinchonidine for 60 min on bimetallic PtAu films are presented in Figure 5 for increasing Pt film thickness. This time is sufficient to observe all adsorbed species and equilibration between species.[9] The signals at 1612, 1590, 1569, 1530, and 1509 cm^{-1} are attenuated upon decrease of the Pt content. The signal at ca. 1455 cm^{-1} is observed with all samples, which might indicate that the quinuclidine moiety is always involved in the adsorption process through the N-atom, irrespective of whether the cinchona alkaloid is adsorbed flat or tilted.[20,22] Note that experiments with cinchonidine adsorbed on monometallic Pt (and also Pd) with metal film thickness below 1 nm showed only very weak features of the alkaloid compared to Pt10 and to the corresponding bimetallic PtAu samples. As a consequence, the spectra of Pt02 and Pt05 are not shown here. A closer look at the spectra in Figure 5 reveals that the way the aforementioned signals decrease on PtAu is not identical for all species. Figure 6A displays the integrated area of the signals associated with the flat (1569 cm^{-1}) and tilted (1509 cm^{-1}) species as a function of Pt thickness. The ratio of the areas of the two signals (hereafter A_{1569}/A_{1509}) is also given assuming that the area is proportional to the relative population of the species. At this point some considerations are needed concerning the band integration. At first, it is likely that the intensity is affected by an enhancement effect, well-known for Au and other noble metals. An absolute assessment of the A_{1569}/A_{1509} ratio cannot be made. Nevertheless, an internal ratio taken across a single spectrum should provide at least a qualitative measure. Next, although the envelope that these signals belong to is complex, the trends shown in Figure 6A demonstrate that the integration is correct in first approximation. Finally, cinchonidine adsorbs also on Au, introducing a source of error. Since PtAu surfaces probably expose also portions of Au at low Pt content, the contribution of the adsorption of cinchonidine on Au should be accounted for when integrating the signal at 1509 cm^{-1}. However, it is assumed here that the free portion of Au capable of adsorbing cinchonidine is far smaller than that in the Au10 sample so that the signals observed on PtAu02 can be attributed predominantly to cinchonidine adsorbed on Pt. This assumption is corroborated by the observation on the same PtAu02 sample

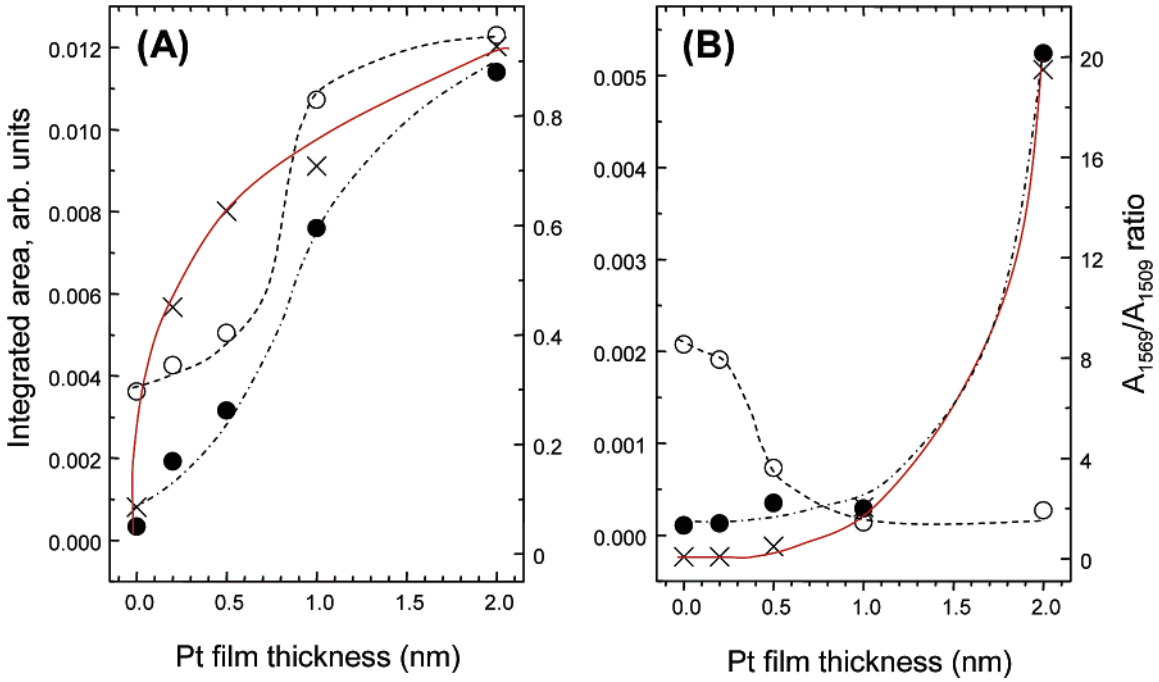

Figure 6. (A) Integrated area of the signals associated with the tilted (1509 cm^{-1}, ○) and the flat (1569 cm^{-1}, ●) species and of the A_{1569}/A_{1509} ratio (×) as a function of Pt film thickness (A) during adsorption and (B) after flowing H_2-saturated solvent for 30 min. Lines are drawn to guide the eye.

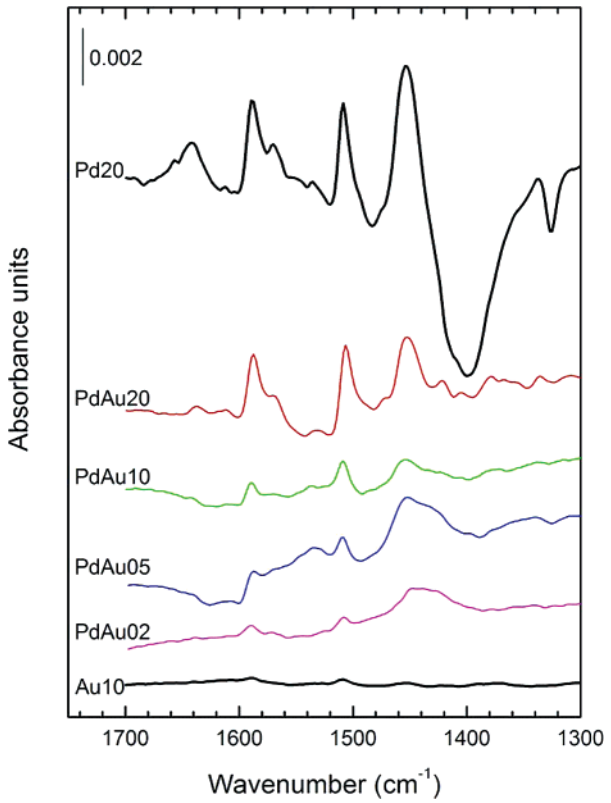

Figure 7. ATR-IR spectra of cinchonidine on monometallic Au and Pd (bold) and on bimetallic PdAu. Conditions: $t = 60$ min, $C_{CD} = 0.1$ mM, 10 °C, H_2-saturated CH_2Cl_2.

of α-quinolyl species (1530 cm^{-1}), which adsorbs only on Pt. It is further demonstrated in Figure 6A, where the amount of tilted species on PtAu02 is higher than on Au10.

With these considerations in mind, Figure 6A shows that both flat and tilted species increase with Pt content. However, the simultaneous increase of the A_{1569}/A_{1509} ratio reveals that the flat species is favored at high Pt content, whereas the tilted species dominates at low Pt content and on Au. Equivalent information is obtained when the signals associated with the two species on PtAu samples were also integrated after flowing H_2-saturated solvent for 30 min (Figure 6B). The fraction of flat species increases with Pt thickness as clearly shown by the A_{1569}/A_{1509} ratio. The opposite behavior of the two species shown in Figure 6B indicates that the flat species is more strongly adsorbed than the tilted species, similarly to the monometallic Pt surface. However, the adsorption equilibrium is shifted toward the tilted species at low Pt content.

Beside the difference in adsorption strength between species on the same metal, the adsorbed layer on Au, which is composed of tilted-like species, appears more strongly bound than the tilted species on Pt. This observation is confirmed by the stability of the signal at 1509 cm^{-1} on Au toward flowing solvent (Figures 3b and 6B), which contrasts with the removal of the majority of the tilted species from monometallic Pt, PtAu10, and PtAu20 samples.

The typical features of adsorbed cinchonidine on Pt are also found on Pd except for the relative ratio of the signals at 1570 and 1508 cm^{-1}, which is very similar to that observed for cinchonidine in solution (Figure 7 and Table 1). This is the major difference between adsorption on the two platinum metals and was attributed to the fact that the tilted species of the alkaloid dominates on Pd.[24] It is obvious from Figure 7 that the intensity of all signals decreases with Pd film thickness in bimetallic

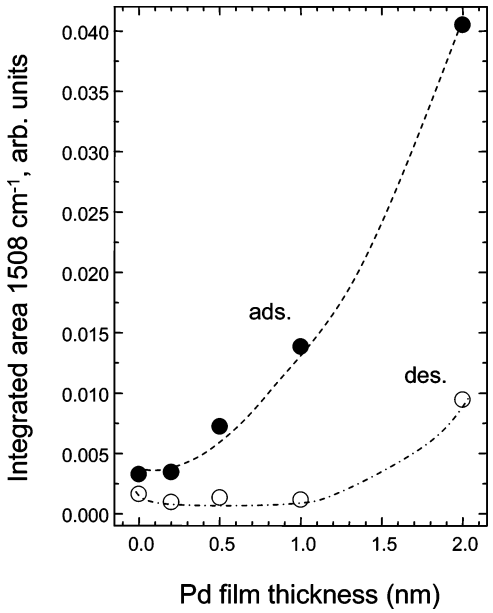

Figure 8. Integrated area of the signal associated with tilted species during cinchonidine adsorption (●) and after flowing H_2-saturated solvent for 30 min (○) as a function of Pd film thickness in bimetallic PdAu. Lines are drawn to guide the eye.

PdAu samples, indicating that the fraction of cinchonidine adsorbed tilted on Pd diminishes with decreasing Pd content.

It is worthwhile mentioning here that the difference in the intensity of all signals on Pd20 compared to the PdAu20 samples is likely due to the partial dilution of Pd in the Au film as schematically shown in Figure 2.[33] This dilution results in Pd ensembles which are smaller than those existing in the corresponding monometallic films.

Figure 8 illustrates the effect of changing Pd film thickness on the integrated areas of the signal at 1508 cm^{-1}, which is representative of the majority of the species present on Pd. During adsorption and when flowing H_2-saturated solvent for 30 min, the fraction of adsorbed cinchonidine increases with Pd film thickness. It is also found that the adsorbed layer of cinchonidine remaining on the Pd-containing surfaces after solvent flow has a comparable stability to that remaining on Au. However, the origin of this stability is different on the two metals.

Discussion

The behavior of the quinoline ring of cinchonidine on Au is in agreement with the vertical and/or tilted adsorption mode of N-heteroaromatic molecules on this metal. Isoquinoline,[48] 8-hydroxyquinoline,[49] and pyridine[50−53] exhibit such an adsorption mode on single-crystal surfaces with tilting angles of up to 70°. Interestingly, polycrystalline surfaces also allow for parallel geometries,[54] a behavior attributed to the presence of defects. The present DFT calculations provide an explanation for this adsorption geometry based on the very weak bonding of quinoline on Au. This behavior is attributed to two joint factors, the degrees of overlap of the orbitals of the adsorbate with the d orbitals of Au and the degree of filling of the antibonding states.[55]

The ATR-IR spectra demonstrate that cinchonidine readily adsorbs on gold surfaces and forms a fairly stable adsorbed layer. The information contained in the spectra is very similar to that observed on Pd at least with respect to the quinoline ring, which is not oriented parallel to the surface. The spectrum in Figure 3c does not indicate formation of species with the aromatic ring

parallel to the Au surface, though their presence might also depend on solute concentration and hence on surface coverage. The theoretical calculations give comparable adsorption energies for local geometries with the quinoline ring adsorbed flat and tilted with respect to the metal.

The stability of the adsorbed layer formed by cinchonidine on the polycrystalline Au surface somehow stands in contrast to the weak adsorption of quinoline. This behavior is traced to the molecular structure of the alkaloid that has a propensity to form intermolecular interactions both in the liquid[56] and in the solid state.[57] Intramolecular OH−N(quinuclidine) hydrogen bonds are responsible for the formation of "chains of [cinchonidine] molecules along alternate screw axes in the solid state".[57] These lateral interactions seem to dominate over the weak interaction between Au and the quinoline ring thus generating a stable adsorbed layer, whose overall adsorption energy is increased compared to that of the single molecule. The assignment of the signal at ca. 3240 cm^{-1} in the spectrum of cinchonidine on Au to the fingerprint of hydrogen bonding within the adsorbed layer is tempting. However, the contribution of the restructuring of the water layer on the Au surface upon adsorption of the alkaloid is probably dominant and in fact observed already in the case of quinoline. The higher intensity observed in the case of cinchonidine is in agreement with a larger perturbation of the water layer and hence with a denser adsorbed layer of the alkaloid. Whether ordered structures are formed as a result of intermolecular interactions cannot be concluded from our ATR-IR study and should be addressed by using other techniques such as STM or LEED. This possibility cannot be excluded a priori since pyridine is capable of assembling long range ordered structures on Au(111) surfaces.[50] This does not hold true for quinoline and the formation of ordered structures of cinchonidine on Cu(111) is still debated.[58,59] The much lower intensity of the signals of cinchonidine on Au compared to adsorption on Pt (and Pd) indicates not only that the bonding of cinchonidine is weaker than that on the catalytically relevant metals but also that the amount of adsorbed alkaloid is lower on Au. This observation would rather suggest that on Au cinchonidine forms molecular aggregates of variable size organized in the form of islands. Within these islands, the single molecules are statistically oriented with the quinoline ring nonparallel to the surface and with the quinuclidine moiety involved in hydrogen bonds with adjacent molecules. Since the nature of the bonding of the single molecule within the island is significantly different from the bonding of cinchonidine with Pt and Pd, the single species forming the island cannot be properly named "tilted" as is the case on the enantioselective hydrogenation metals.

This work indicates that a phase transition between single molecule chiral sites and "condensation" of aggregates on the surface can be expected when passing from Pt or Pd to Au.

On the catalytically relevant metals, the transition from a local adsorption geometry in which the quinoline ring is predominantly adsorbed flat to one in which it is tilted away from the metal surface depends on the degree of interaction of the aromatic ring with the metal surface. This interaction can be affected by the size of the metal domains on which adsorption occurs. In the present study the size of platinum group metal domains has been changed by the use of Au-containing Pt and Pd films. We could show that this size alters the way the chiral modifier coordinates to the surface. This property is probably crucial for understanding the structure sensitivity of supported metals used in enantioselective hydrogenations.[60]

Adsorption of cinchonidine on bimetallic PtAu and PdAu surfaces strongly depends on the metal film thickness and on the composition of the surface. On the monometallic Pt and Pd films adsorption of cinchonidine is very dissimilar from that shown in Figures 5 and 7, in the sense that the ATR-IR spectra for Pt films below 1 nm do not provide any information on adsorbates compared to the bimetallic films. The likely reason for this phenomenon is the enhancement effect offered by the combination of the two metal films. Beside Pt giving moderate enhancement,[34,61,62] Au is an excellent substrate for surface-enhanced infrared absorption (SEIRA) spectroscopy.[63]

CO adsorption on the bimetallic PdAu thin model films used for cinchonidine adsorption strongly indicated that the size of the Pd ensembles which are able to adsorb the probe molecule are smaller compared to those present in the monometallic Pd surfaces. This has been explained in terms of formation of a diffuse Pd/Au interface, which makes the active Pd particles smaller.[33] This dilution effect is in agreement with the tendency of Pd−Au bimetallic surfaces to form alloys even at ambient temperature.[64,65] On the other hand, formation of Pt−Au ensembles in PtAu thin model films is more difficult[66] and segregation of the two metals is favored to some extent. This results in comparable CO spectra in mono- and bimetallic samples.[33] The diffuse interface is likely reflected in the adsorption of cinchonidine. Figure 5 reveals that there is not much difference in intensity between the spectrum of cinchonidine on Pt10 and on PtAu10. On the contrary, Figure 7 shows that the spectrum of the alkaloid on PdAu20 is attenuated by about 30% with respect to that of the Pd20 sample, indicating that a smaller fraction of cinchonidine is adsorbed on the PdAu20 sample owing to the reduced size of the free Pd ensembles. Hence, the use of Au is revealed to better simulate a particle size effect than simply reducing the film thickness of the noble metal.

It is important to emphasize that the changes in the distribution of the species of cinchonidine on PtAu are much more significant than the changes observed in CO adsorption on the same surfaces.[33] The fraction of flat species appears larger at high Pt content, whereas the fraction of tilted species increases with decreasing Pt content. It is obvious that flat species require more Pt atoms to adsorb, since they exhibit a larger cross section than tilted species due to the extended aromatic ring. Hence, cinchonidine appears a better probe to characterize the PtAu bimetallic surfaces because it is more sensitive to the size of the Pt ensembles than CO, which adsorbs mainly on-top on Pt.[33,34] CO is a good candidate for the PdAu samples because it forms multibonded species on Pd. On the other hand, only tilted species can be observed in the case of adsorption of cinchonidine, which are less sensitive to the size of the metal ensembles.

Conclusions

The adsorption of the chiral modifier cinchonidine from CH_2Cl_2 solvent has been investigated with ATR-IR spectroscopy on monometallic Au and on bimetallic Pt−Au and Pd−Au thin model films. The spectroscopic data indicate that on Au cinchonidine adsorbs with the quinoline ring nonparallel to the surface and that the alkaloid adsorbs more strongly than quinoline. DFT calculations indicate that the quinoline ring, the anchoring group of cinchonidine, does not form σ-bonds with Au in contrast to Pt. The difference in adsorption strength observed with respect to quinoline and the comparable adsorption energy calculated for flat and tilted quinoline on Au suggest that hydrogen bond-type interactions stabilize the adsorbed cinchonidine layer. These intermolecular interactions likely favor

the formation of cinchonidine islands on Au in which the single molecule chirality likely responsible for the enantioselective properties of cinchona modified platinum metals is broken.

On bimetallic Pt−Au thin model films the population of flat species (irreversibly adsorbed) decreases with decreasing Pt film thickness and quinoline ring tilting prevails at very low Pt content. Evaporation of Au before Pt and Pd generates bimetallic surfaces where the role of Au is to modify the effective ensemble size of the noble metal. This modification allows the enhancement of the information that can be gained by simply changing Pt (and Pd) thickness in the absence of Au. In this respect, due to its relatively large molecular size cinchonidine appears a better candidate than CO to probe the ensemble size of Pt−Au films. Cinchonidine seems to prefer a tilted local geometry on very small Pt ensembles, whereas on larger ensembles flat adsorption is favored.

The results obtained on the Pt−Au bimetallic surfaces provide evidence for the sensitivity of the adsorption geometry of the chiral modifier on the size of metal ensembles. This property likely plays an important role in the heterogeneous enantioselective hydrogenation over chirally modified platinum group metals.

Acknowledgment. The authors gratefully acknowledge financial support from the Swiss National Science Foundation and the Foundation Claude and Giuliana, and the computing time provided by the Swiss Center for Scientific Computing (SCSC) in Manno.

References and Notes

(1) Kacprzak, K.; Gawronski, J. *Synthesis* **2001**, 961.
(2) Bürgi, T.; Baiker, A. *Acc. Chem. Res.* **2004**, *37*, 909.
(3) Murzin, D. Y.; Mäki-Arvela, P.; Toukoniitty, E.; Salmi, T. *Catal. Rev.* **2005**, *47*, 175.
(4) Vargas, A.; Bürgi, T.; Baiker, A. *J. Catal.* **2004**, *226*, 69.
(5) Diezi, S.; Mallat, T.; Szabo, A.; Baiker, A. *J. Catal.* **2004**, *228*, 162.
(6) Bonalumi, N.; Vargas, A.; Ferri, D.; Bürgi, T.; Mallat, T.; Baiker, A. *J. Am. Chem. Soc.* **2005**, *127*, 8467.
(7) Carley, A. F.; Rajumon, M. K.; Roberts, M. W.; Wells, P. B. *J. Chem. Soc., Faraday Trans.* **1995**, *91*, 2167.
(8) Evans, T.; Woodhead, A. P.; Gutierrez-Sosa, A.; Thornton, G.; Hall, T. J.; Davis, A. A.; Young, N. A.; Wells, P. B.; Oldman, R. J.; Plashkevych, O.; Vahtras, O.; Agren, H.; Carravetta, V. *Surf. Sci.* **1999**, *436*, L691.
(9) Ferri, D.; Bürgi, T. *J. Am. Chem. Soc.* **2001**, *123*, 12074.
(10) Chu, W.; LeBlanc, R. J.; Williams, C. T. *Catal. Commun.* **2002**, *3*, 547.
(11) Kubota, J.; Ma, Z.; Zaera, F. *Langmuir* **2003**, *19*, 3371.
(12) Chu, W.; LeBlanc, R. J.; Williams, C. T.; Kubota, J.; Zaera, F. *J. Phys. Chem. B* **2003**, *107*, 14365.
(13) Attard, G. A. *J. Phys. Chem. B* **2001**, *105*, 3158.
(14) Bakos, I.; Szabo, S.; Bartok, M.; Kalman, E. *J. Electroanal. Chem.* **2002**, *532*, 113.
(15) von Arx, M.; Wahl, M.; Jung, T. A.; Baiker, A. *Phys. Chem. Chem. Phys.* **2005**, *7*, 273.
(16) Bonello, J. M.; Lambert, R. M. *Surf. Sci.* **2002**, *498*, 212.
(17) LeBlanc, R. J.; Chu, W.; Williams, C. T. *J. Mol. Catal. A*: *Chem.* **2004**, *212*, 277.
(18) LeBlanc, R. J.; Williams, C. T. *J. Mol. Catal. A: Chem.* **2004**, *220*, 207.
(19) Ma, Z.; Zaera, F. *J. Phys. Chem. B* **2005**, *109*, 406.
(20) Vargas, A.; Ferri, D.; Baiker, A. *J. Catal.* **2005**, *236*, 1.
(21) Vargas, A.; Baiker, A. *J. Catal.* **2006**, *239*, 220.
(22) Calvo, S. R.; LeBlanc, R. J.; Williams, C. T.; Balbuena, P. B. *Surf. Sci.* **2004**, *563*, 57.
(23) Bonello, J. M.; Lindsay, R.; Santra, A. K.; Lambert, R. M. *J. Phys. Chem. B* **2002**, *106*, 2672.
(24) Ferri, D.; Bürgi, T.; Baiker, A. *J. Catal.* **2002**, *210*, 160.
(25) Mallat, T.; Szabo, S.; Schürch, M.; Göbel, U. W.; Baiker, A. *Catal. Lett.* **1997**, *47*, 221.
(26) Haruta, M.; Daté, M. *Appl. Catal. A* **2001**, *222*, 427.
(27) Claus, P. *Appl. Catal. A* **2005**, *291*, 222.
(28) Sinfelt, J. H. *Acc. Chem. Res.* **1977**, *10*, 15.
(29) Chen, M.; Kumar, D.; Yi, C. W.; Goodman, D. W. *Science* **2005**, *310*, 291.
(30) Jones, T. E.; Noakes, T. C. Q.; Bailey, P.; Baddeley, C. J. *Surf. Sci.* **2004**, *569*, 63.
(31) Jones, T. E.; Noakes, T. C. Q.; Bailey, P.; Baddeley, C. J. *J. Phys. Chem. B* **2004**, *108*, 4759.
(32) Osawa, T.; Harada, T.; Takayashu, O. *Top. Catal.* **2000**, *13*, 155.
(33) Behzadi, B.; Ferri, D.; Kappenberger, P.; Hauert, R.; Ernst, K. H.; Baiker, A. Manuscript in preparation.
(34) Ferri, D.; Bürgi, T.; Baiker, A. *J. Phys. Chem. B* **2001**, *105*, 3187.
(35) Baerends, E. J.; Autschbach, J.; Berces, A.; Bo, C.; Boerrigter, P. M.; Cavallo, L.; Chong, D. P.; Deng, L.; Dickson, R. M.; Ellis, D. E.; Fan, L.; Fischer, T. H.; Guerra, C. F.; van Gisbergen, S. J. A.; Groeneveld, J. A.; Gritsenko, O. V.; Gröning, M.; Harris, F. E.; van den Hoek, P.; Jacobsen, H.; van Kessel, G.; Kootstra, F.; vanLenthe, E.; Osinga, V. P.; Patchkovskii, S.; Philipsen, P. H. T.; Post, D.; Pye, C. C.; Ravenek, W.; Ros, P.; Schipper, P. R. T.; Schreckenbach, G.; Snijders, J. G.; Sola, M.; Swart, M.; Swerhone, D.; te Velde, G.; Vernooijs, P.; Versluis, L.; Visser, O.; van Wezenbeek, E.; Wiesenekker, G.; Wolff, S. K.; Woo, T. K.; Ziegler, T. *ADF−Amsterdam Density Functional*; Release 2004-01 ed.; Scientific Computing and Modelling NV, Vrije Universiteit,Theoretical Chemistry: Amsterdam, The Netherlands.
(36) van Lenthe, E.; Baerends, E. J.; Snijders, J. G. *J. Chem. Phys.* **1993**, *99*, 4597.
(37) van Lenthe, E.; Baerends, E. J.; Snijders, J. G. *J. Chem. Phys.* **1994**, *101*, 9783.
(38) van Lenthe, E.; Baerends, E. J.; Snijders, J. G. *J. Chem. Phys.* **1996**, *105*, 6505.
(39) van Lenthe, E.; van Leeuwen, R.; Baerends, E. J.; Snijders, J. G. *Int. J. Quantum Chem.* **1996**, *57*, 281.
(40) van Lenthe, E.; Baerends, E. J.; Snijders, J. G. *J. Chem. Phys.* **1999**, *110*, 8943.
(41) Becke, A. D. *Phys. Rev. A* **1988**, *38*, 3098.
(42) Perdew, J. P. *Phys. Rev. B* **1986**, *33*, 8822.
(43) Versluis, L.; Ziegler, T. *J. Chem. Phys.* **1988**, *88*, 322.
(44) Fan, L.; Ziegler, T. *J. Chem. Phys.* **1991**, *95*, 7401.
(45) Bonalumi, N.; Vargas, A.; Ferri, D.; Baiker, A. Manuscript in preparation.
(46) Khein, A.; Singh, D. J.; Umrigar, C. J. *Phys. Rev. B* **1995**, *51*, 4105.
(47) Schaftenaar, G.; Noordik, J. H. *J. Comput.-Aided Mol. Des.* **2000**, *14*, 123.
(48) Yang, D.-F.; Lipkowski, J. *Langmuir* **1994**, *10*, 2647.
(49) Kim, S.; Joo, S. W. *Vib. Spectrosc.* **2005**, *39*, 74.
(50) Cai, W. B.; Wan, L. J.; Noda, H.; Hibino, Y.; Ataka, K.; Osawa, M. *Langmuir* **1998**, *14*, 6992.
(51) Hoon-Khosla, M.; Fawcett, W. R.; Chen, A.; Lipkowski, J.; Pettinger, B. *Electrochim. Acta* **1999**, *45*, 611.
(52) Ikezawa, Y.; Sawatari, T.; Terashima, H. *Electrochim. Acta* **2001**, *46*, 1333.
(53) Ikezawa, Y.; Kosugi, T. *Electrochim. Acta* **2002**, *47*, 2921.
(54) Ikezawa, Y.; Sawatari, T.; Kitazume, T.; Goto, H.; Toriba, K. *Electrochim. Acta* **1998**, *43*, 3297.
(55) Hammer, B.; Norskov, J. K. *Nature* **1995**, *376*, 238.
(56) Ferri, D.; Bürgi, T.; Baiker, A. *J. Chem. Soc., Perkin Trans. 2* **1999**, 1305.
(57) Oleksyn, B. J. *Acta Crystallogr.* **1982**, *B38*, 1832.
(58) Xu, Q.-M.; Wang, D.; Wan, L.-J.; Bai, C.-L.; Wang, Y. *J. Am. Chem. Soc.* **2002**, *124*, 14300.
(59) Friebel, D.; Mangen, T.; Obliers, B.; Schlaup, C.; Broekmann, P.; Wandelt, K. *Langmuir* **2004**, *20*, 2803.
(60) Wehrli, J. T.; Baiker, A.; Monti, D. M.; Blaser, H. U. *J. Mol. Catal.* **1990**, *61*, 207.
(61) Nakao, Y.; Yamada, H. *Surf. Sci.* **1986**, *176*, 578.
(62) Nakamura, R.; Sato, S. *Langmuir* **2002**, *18*, 4433.
(63) Osawa, M. *Bull. Chem. Soc. Jpn.* **1997**, *70*, 2861.
(64) Koel, B. E.; Sellidj, A.; Paffett, M. T. *Phys. Rev. B* **1992**, *46*, 7846.
(65) Schmidt, T. J.; Stamenkovic, V.; Arenz, M.; Markovic, N. M.; Ross, P. N. *Electrochim. Acta* **2002**, *47*, 3765.
(66) Bouwman, R.; Sachtler, W. M. H. *J. Catal.* **1970**, *19*, 127.